Solid Earth Discuss., 5, 897–916, 2013
www.solid-earth-discuss.net/5/897/2013/
doi:10.5194/sed-5-897-2013

Solid Earth
Discussions
Open Access

Time dependent properties of sandstones and their effects on mine stability

M. Alber

Ruhr-University Bochum, Germany

Received: 26 March 2013 – Accepted: 5 June 2013 – Published: 3 July 2013

Correspondence to: M. Alber (michael.alber@rub.de)

Published by Copernicus Publications on behalf of the European Geosciences Union.

Abstract

Large scale stress redistribution around longwall panels in coal mines puts rock masses in the vicinity of the underground excavations close to failure. While immediate failure is reflected for example by instantaneous seismic events, there is also a delayed response of the rock mass as noted from decaying seismicity during non-operating times. Sandstone samples from the hanging wall of a coal seam in the Ruhr coal mining district in Germany have been subjected to conventional strength, creep and relaxation tests. From creep and relaxation tests estimates of time dependent strength properties are derived. Numerical modeling was employed to delineate zones of states of stress around underground excavations which are prone to time dependent failure.

1 Introduction

Typically only significant mining-induced seismic events are investigated for their impact on mine and environmental safety although smaller events may offer insight into the strength of the uppermost crust. Seismic events may be classified according to failure processes involved during mining. As shown in Fig. 1, Ortlepp (1992) distinguished two different types of failures of the geologic media and assigned typical magnitudes to those failures. Large mining induced seismic events ($ML > 2$) typically are associated with shear failure and fault reactivation. Ortlepp's experience from South Africa has been confirmed for large seismic events in German coal mining (Alber and Fritschen, 2011). Events of smaller magnitudes ($ML < 2$) could also be associated with failure of hanging walls and similar local failure processes (Alber et al., 2009). However, Bischoff et al. (2010) recorded seismic events in the same coal mine and clearly showed diminishing seismic events on weekends (non-operative times); i.e. the events did not stop immediately after excavation. The temporal pattern of seismic events reflects the time dependent behavior of rock under excavation- induced stress changes.

There exists a vast body of knowledge on time dependent behavior of rock salt as well as many theoretical approaches towards that problem (Cristescu, 1993) but little is known for hard rocks. Applied research on that topic is mainly executed in South Africa (Drescher, 2002; Malan, 1999) for evaluating time dependent tunnel closure in the deep mines in hard rock. Recently, Damanjac and Fairhurst (2010) discussed an estimate of the time independent (infinite long term) strength for the Lac du Bonnet granite in the range of 45 % of the unconfined compressive strength (UCS).

This paper focuses on time dependent rock behavior around a deep longwall coal mine in the Ruhr mining district, Germany with the goal of identifying the volume of a rock mass that is prone to failure within a few days. Rock samples were collected by underground drilling; the rocks were thoroughly characterized and subjected to conventional strength tests, uniaxial relaxation and creep tests.

2 Stress redistribution around underground excavations and seismic events

When extracting coal reserves by the longwall mining method, huge underground openings of large dimensions are created. The place of extraction, the longwall face, is protected by shields and when these move ahead the hanging strata fails, involving tensile and shear failure processes. These failure processes reach up to appoximately 10 times the seam height and are close to the excavation perimeter. The failure processes are documented in immediate seismic events. However, as shown by Bischoff et al. (2010) there are seismic events after the actual excavation stops. This was observed for a number of events over the week (Fig. 1a) as well as over the working day (Fig. 1b). There are neither excavation works during the weekends nor during the night hours.

Further analysis demonstrates that this pattern holds true for any month of a year-long longwall operation at the same mine. Figure 2a, b shows two selected months of 2007 and clearly there are diminishing magnitudes over the weekends. Longer breaks in mining (holiday breaks) also show clearly lower yet persisting magnitudes.

SED
5, 897–916, 2013

This seismic signature was interpreted as a delayed rock mass response to excavation and may serve as a calibration for the estimation of time dependent strength of rock at the mine. The typical approach to mine design involves a comparison of stresses with static rock strength. In the presented case however a time-dependent rock behavior may be assumed where the strength of the rocks decreases and fails well after being subjected to excavation induced stresses. The time span of interest here is in the order of a few days.

The state of stress (and strain) around the longwall panel at the mine was computed with the 3-D boundary element code EXAMINE^{3D} (Rocscience, 1997) using the following input data:

$\sigma_v = 28.6$ MPa. $\sigma_H = 40$ MPa, $\sigma_h = 18$ MPa. The typical rock mass strength is given by the uniaxial compressive rock strength $\sigma_C = 100$ MPa and the Hoek–Brown parameters $s = 0.0286$ and $m = 5.5$ and the elastic parameters are Young's Modulus $E = 17$ GPa and Poisson's ratio $\nu = 0.25$, repectively (Alber et al., 2009). The longwall at depth 1100 m below surface has dimensions of $w \times l \times h = 300\,\mathrm{m} \times 1050\,\mathrm{m} \times 3\,\mathrm{m}$ and its long axis is parallel to σ_H. The elastic numerical model suggests the limits of the overstresses (i.e. broken) rock of approximately 30 m height above the centre of excavation and few meters at the rim of the excavation. This result is confirmed by in situ observations. There is a transition from a broken rock mass above the excavation to a stable yet highly strained rock mass around the excavation. With the alignment of the long axis of the longwall parallel to σ_H the highest strain concentrations in the stable rock may be found along the side abutments of the longwall. Figure 3a and b suggest uniaxial strain conditions at the side abutments. It is at these locations that the rock mass is assumed will fail after some time.

3 Laboratory deformation tests on time dependent behavior of rock

Rock cores from the hanging strata of that longwall comprise fine- and medium-grained sandstones as well as coarse siltstones. Rock mechanical tests include uniaxial com-

SED
5, 897–916, 2013

pressive strength tests, relaxation and creep tests to evaluate the rock's ability to sustain uniaxial deformation for a few days. The following sections focus on the behavior of a typical hanging wall rock, a fine-grained sandstone.

3.1 Uniaxiale compressive tests (UCS)

These tests allow for the estimation of uniaxial strength from fast deformation tests with an axial strain rate as suggested by the International Society of Rock Mechanics (Ulusay and Hudson, 2007) $\dot{\varepsilon}_a = 10^{-5}\,\mathrm{mm\,mm^{-1}\,s^{-1}}$, i.e. the samples failed within 10–15 min. Moreover, Young's Modulus E, Poisson's ratio ν, lateral ε_l and volumetric strain ε_v as well as the crack volumetric strain ε_{cv} (Lajtai, 1998) were used to evaluate onset of crack initiation and crack sliding, respectively. The following formulas were used:

$$\varepsilon_v = \varepsilon_a + 2\varepsilon_l \tag{1}$$

$$\varepsilon_{cv} = \varepsilon_v - \frac{\sigma_a(1-2\nu)}{E} \tag{2}$$

3.2 Relaxation tests

The relaxation tests were conducted on cylindrical specimens with $L/D = 2/1$ and $D = 40\,\mathrm{mm}$ in a stiff loading frame using a MTS Teststar IIm controller. The specimens were loaded with a strain rate control up to preset axial strain level ε_{a1} und left until the axial stress σ_a relaxed to a constant level. The necessary period of time for complete relaxation was typically below 30 min. Then, the specimen was deformed to the next axial strain level ε_{a2} and relaxed again. This procedure was repeated until the sample failed. Recorded data include time, axial strain ε_a and stress σ_a as well as the lateral strain ε_l. Figure 4 depicts an example of a 6-stage relaxation test on sandstone. It may be seen that for each deformation stage ε_a the sample relaxes within 2000 s to a constant axial stress level σ_a. At the last stage at $\varepsilon_{a6} = 750$ microstrains (µs) the sample fails after a short time. Also shown is the development of the lateral strain ε_l during this deformation experiment. The lateral strain is plotted positive for convenience.

SED
5, 897–916, 2013

3.3 Creep tests

Creep tests were conducted on cylinders with dimensions $L/D = 2/1$ and $D = 40$ mm in a specifically designed and built loading frame. After placing the samples in the purely mechanical operating loading frame, the preset load was achieved by putting weights on a lever system and the hydraulic ram was lowered on the sample. Recorded data include time, axial strain ε_a and lateral strain ε_l. For the time period of interest as discussed in the introduction, each loading stage σ_a was held constant for at least 2–4 days, and then the next load level was applied. The procedure was repeated until the sample failed. Figure 5 depicts an example of a 7-stage creep test on a sandstone sample. It may be seen that for each loading stage σ_a the sample reacts with a fast axial strain (ε_a) response and then barely deforms. Only at higher loads does the sample accumulate axial strain. Also shown is the development of the lateral strain ε_l during this deformation experiment. The lateral strain is plotted positive for convenience.

3.4 Results of lab tests

3.4.1 Uniaxial compressive tests

Numerous UCS (no. 128) tests were conducted and the average results are given in Table 1. All tested rocks were analyzed for their critical extension strain (Stacey, 1981) which is a strain criterion for fracture in brittle rocks. It works as follows: when plotting the lateral strain ε_l vs. axial strain ε_a a distinct non-linearity may be observed at around 30–40 % of the axial strain at failure. This is the critical extension strain at which fracturing is initiated and which is deemed an important level for subsequent time dependent deformation. Figure 6 shows lateral strain vs. axial strain curves of 27 UCS tests on fine-grained sandstones and the critical extension strain is in the range of $\varepsilon_{l,\,crit} = 0.002$.

SED
5, 897–916, 2013

3.4.2 Relaxation tests

The relaxation tests show that the deformation processes of the samples at constant strain levels are fast. For most strain levels the stresses relaxed within 30 min to a constant level while the sample deformed laterally or, at high axial strains, the sample failed completely. One might conclude that for rocks in mining conditions defined by constant strain levels the deformation occurs rapidly and failure may take place within 30 min but will not lead to significant delayed response within 2–4 days as the stresses are already released. The strained rock may, however, undergo creep deformation as discussed in the next section.

3.4.3 Creep tests

These test showed a consistent pattern: at lower stress levels there was an instantaneous response of axial strain (and of the lateral strain in a barely detectable level) followed by stable deformation, i.e. little time-dependent change. At low stress levels the deformation rates are very low with $\dot{\varepsilon}_a \approx 10^{-9}$ mm mm^{-1} s^{-1} and $\dot{\varepsilon}_l \approx 10^{-10}$ mm mm^{-1} s^{-1}, respectively. At levels above 70 % of the failure load there were typically significant increases in strains observed. Strain rates accelerate up to $\dot{\varepsilon}_a \approx \dot{\varepsilon}_l \approx 10^{-5}$ mm mm^{-1} s^{-1} which are similar levels as in UCS tests. The average creep Young's Modulus $E_C = 17.1$ GPa is much lower than the average static Young's Modulus $E = 24.8$ GPa (cf. Table 1).

3.5 Combined visualization of deformation tests

The data from UCS and creep tests may be further analyzed by computing the volumetric strain ε_v and the crack volumetric strain ε_{cv}. Figure 7 shows a comprehensive graph depicting the various stress-strain data during a creep experiment in comparison to the stress-strain data in a uniaxial compressive strength test. Both samples were from the same core run, i.e. the same sandstone horizon. It may be seen that the stress levels of sample failure (≈ 120 MPa) in UCS test and creep test are similar. The axial strain curves are quite different as it should be when the sample is given time for creep. Young's Moduli are from UCS tests E = 25.2 MPa and from creep test E_C = 14.5 GPa, respectively. The lateral strain curves are of similar shape but in different magnitudes. However, both curves show a clear deviation from linearity in higher stress levels, indicating a significant increase in lateral deformation. This is interpreted as the onset of accelerated creep which may finally lead to failure within a few days.

When observing the curves of the volumetric strain (Fig. 7 bottom) it may be seen that the reversal of the curves is in the order of 70–80 % of the respective volumetric strains at uniaxial compressive strength. This threshold of slope reversal is the onset of instable fracture propagation as defined by Bieniawski (1967) and Martin (1997). This holds also true for the volumetric strain curves from the creep tests. The creep samples under constant loading conditions exhibit higher volumetric strains but their slope reversals are also at 70–80 % of the creep strength.

Analyses of the crack volumetric curves give further insight in the experiments. In the UCS test there is a distinct gap between volumetric and crack volumetric curve, indicating the elastic volumetric strain of the sample. In the creep test however both curves are almost congruent to each other so that no or very little elastic volumetric strain is observed.

In summary, the deformation tests showed that hard brittle rocks exhibit time dependent behavior relevant for short-termed mining applications. The ultimate strengths from UCS, relaxation or creep tests are similar. Above loads of 70–80 % of the ultimate strength the sandstones develop strain rates (axial and lateral) that may lead to failure within a few days. Figure 8 shows the lateral strain rates as function of the axial strain level. A sandstone strained to of 80 % of its maximum axial strain will develop lateral strain rates of $\dot{\varepsilon}_l > 10^{-8}\,\mathrm{mm\,mm^{-1}\,s^{-1}}$. Given the fact that the tested rocks fail at lateral strains of some 0.002 the time to failure is around 55 h or a little over 2 days.

4 Discussion and conclusions

Seismic events after breaks in mining suggest time dependent rock behavior around longwall coal mining operations. Laboratory tests support this notion. First of all, the rocks are strained well beyond the critical extension strain and are thus prone to failure in due course. Stress relaxation of the tested rocks occurs within 30 min at all strain stages. At stress levels below 70 % of the maximum stress the creep processes in the rock does not lead to short-term failure. At axial strain levels of $\varepsilon_a \approx 0.004$ (cf. Fig. 5) the lateral strain rate accelerates and the rock may fail in few days. There exist zones around the longwall where deformation conditions are similar to the lab conditions, i.e. uniaxially strained volumes of rocks (cf. Fig. 2a and b). These rock volumes are subjected to levels of strain allow time dependent deformation processes leading to rock failure within a few days.

The approach to use strain and deformation rates to estimate the time to failure is used for rock slopes (Cruden and Masumzadeh, 1987; Zavodni and Broadbent, 1980) as well as for slopes in soil (Saito and Uzewa, 1961; Saito, 1969). Similar approaches may also be used for estimating the time to failure in underground excavations. First, the critical stress/strain levels for achieving sufficiently high strain rates may be determined from uniaxial creep testing. The corresponding strain rates may also be calculated. The actual states of strain/stress may be evaluated from numerical modeling and the time to failure may be estimated. Analyses of mining induced seismic allow validation of the assumptions.

Acknowledgements. This research has been executed in the context of the Collaborative Research Center CRC 526 “Rheology of the Earth” funded by the German Research Society (DFG) for the period 2008–2011. Their support is gratefully acknowledged.

References

Alber, M. and Fritschen, R.: Rock mechanical analysis of a $M_l = 4.0$ seismic event induced by mining in the Saar District, Germany, Geophys. J. Int., 186, 359–372, 2011.

Alber, M., Fritschen, R., Bischoff, M., and Meier. T.: Rock mechanical investigations of seismic events in a deep longwall coal mine, Int. J. Rock Mech. Min., 46, 408–420, 2009.

Bieniawski, Z. T.: Mechanism of brittle fracture of rock – Part I: Theory of the fracture process, Int. J. Rock. Mech. Min., 4, 395–496, 1967.

Bischoff, M., Cete, A., Fritschen, R., and Meier, T.: Coal mining induced seismicity in the Ruhr area, Germany, Pure Appl. Geophys., 167, 63–75, 2010.

Cristescu, N. D.: Rock rheology, in: Comprehensive Rock Engineering, vol. 1, edited by: Hudson, J. A., 523–544, 1993.

Cruden, D. M. and Masoumzadeh, S.: Accelerating creep of the slopes of coal mine, Rock Mech. Rock Eng., 20, 122–135, 1987.

Damjanac, B. and Fairhurst, C.: Evidence for a long-term strength threshold in crystalline rock, Rock Mech. Rock Eng., 43, 513–531, doi:10.1007/s00603-010-0090-9, 2010.

Drescher, K.: An investigation into the mechanisms of time dependent deformation of hard rocks, Master's Thesis, University of Pretoria, South Africa, 2002.

Examine3D 4.0. Rocscience Inc.: Examine3D Version 4.0 3-D Engineering Analysis for Underground Excavations, Toronto, Ontario, Canada, 1997.

Hellenkamp, T.: Rock mechanical investigations on time-dependent rock deformation around subsurface coal mining (in German), PhD thesis, Ruhr University Bochum, Germany, 2011.

Lajtai, E. Z.: Microscopic fracture processes in a granite, Rock Mech. Rock Eng., 31, 237–250, 1998.

Malan, D. F.: Time-dependent behavior of deep level tabular excavations in hard rock, Rock Mech. Rock Eng., 32, 123–155, 1999.

Martin, C. D.: Seventeenth Canadian geotechnical colloquium: the effect of cohesion loss and stress path on brittle rock strength, Can. Geotech. J., 34, 698–725, 1997.

Ortlepp, W. D.: The design of support for the containment of rockburst damage in tunnels; an engineering approach, in: Proc. Int. Symp. Rock Support, edited by: Kaiser, P. K. and McCreath, D. R., Sudbury, Ontario, Canada, 16–19 June 1992, 593–609, 1992.

Saito, M.: Forecasting time of slope failure by tertiary creep, in: Proc. 7th Conf. Soil Mech. Found. Eng., Mexico City, Mexico, 1969, 677–683, 1969.

Saito, M. and Uezawa, H.: Failure of soil due to creep, in: Proc. 5th Conf. Soil Mech. Found. Eng., San Francisco, 12–16 August 1985, 315–318, 1961.
Stacey, T. R.: A simple extension strain criterion for fracture of brittle rock, Int. J. Rock Mech. Min., 18, 469–474, 1981.
Ulusay, R. and Hudson, J. A. (eds.): The Complete ISRM Suggested Methods for Rock Characterization, Testing and Monitoring: 1974–2006, ISRM, Lisbon, 2007.
Zavodni, Z. M. and Broadbent, C. D.: Slope failure kinematics, CIM Bull., 73, 69–74, 1980.

SED
5, 897–916, 2013
Time dependent effects on mine stability
M. Alber

Table 1. Some properties (average values) of the tested rocks.

Rock type	σ_C (MPa)	ρ ($g\,cm^{-3}$)	v_P ($km\,s^{-1}$)	E (GPa)	ν (–)
Siltstone	100	2.69	4.3	17.6	0.18
Sandstone, fine-grained	111	2.58	4.3	24.8	0.21
Sandstone, coarse-grained	134	2.66	4.4	23.6	0.26

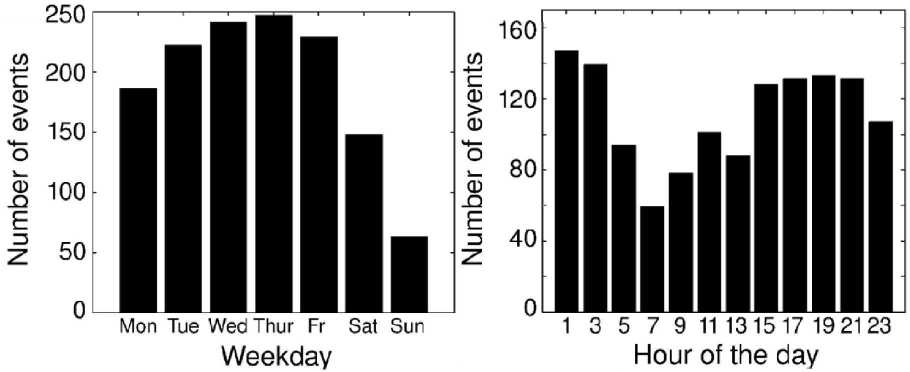

Fig. 1. (a) (left) Number of mining induced seismic events during a working week. **(b)** (right) Number of mining induced seismic events during a working day (Bischoff et al., 2010).

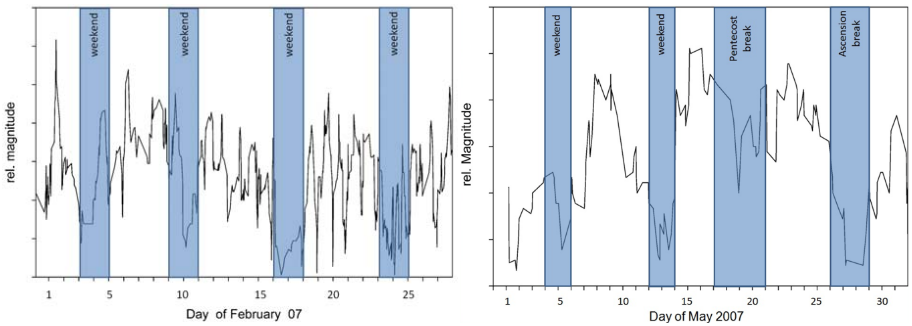

Fig. 2. (a) (left) Magnitudes of mining induced seismic events in February 2007) and **(b)**, (right) May 2007. The plot line is a computed running average of 5 single magnitudes.

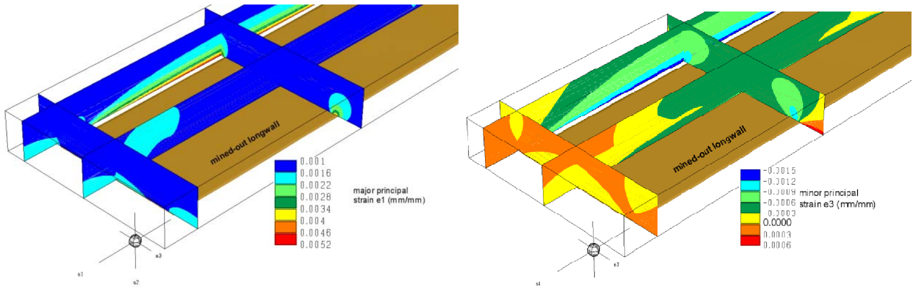

Fig. 3. Major (left) and minor (right) principal strain from 3-D elastic numerical modeling. Volumes of uniaxially strained rock (i.e. minor principal stress = 0) are at the rim of the longwall.

SED
5, 897–916, 2013

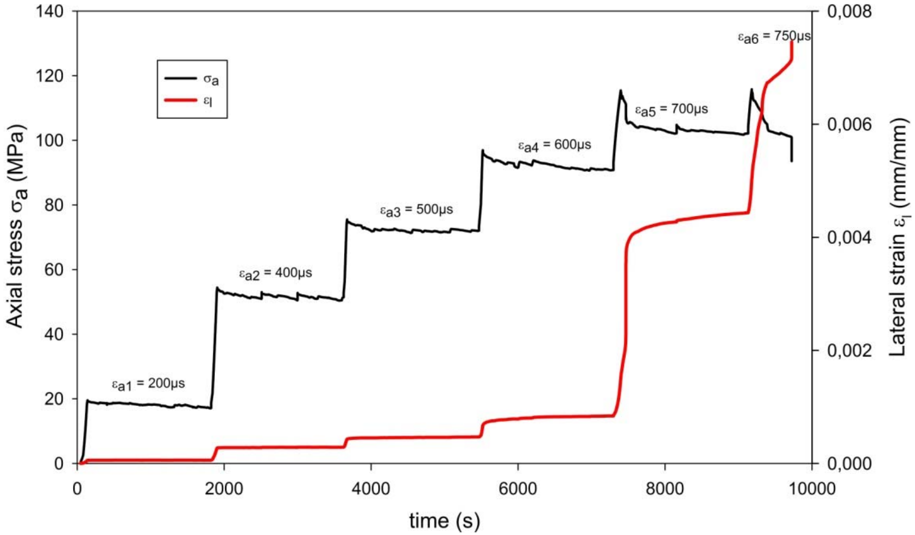

Fig. 4. Example of a 6-stage relaxation test on sandstone.

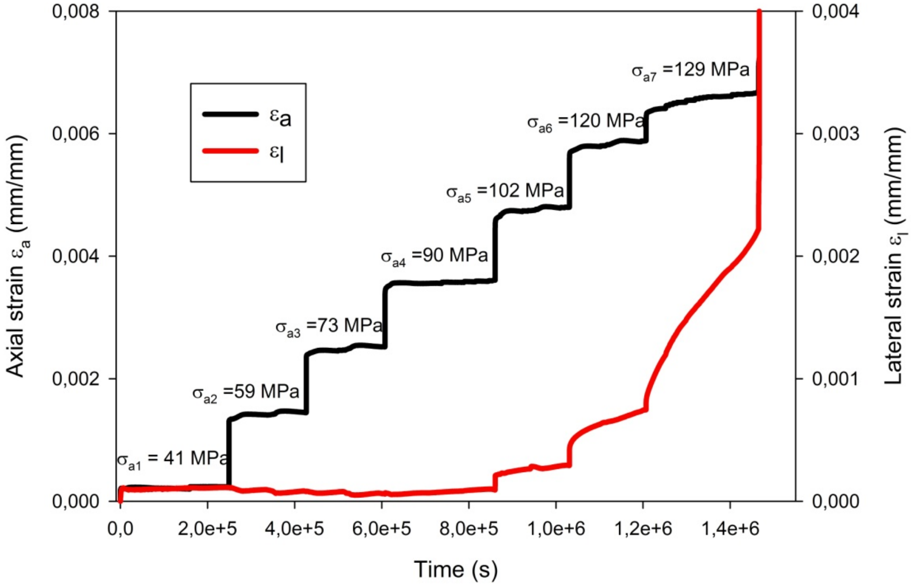

Fig. 5. Example of a multistage creep test on sandstone.

SED
5, 897–916, 2013

Time dependent effects on mine stability

M. Alber

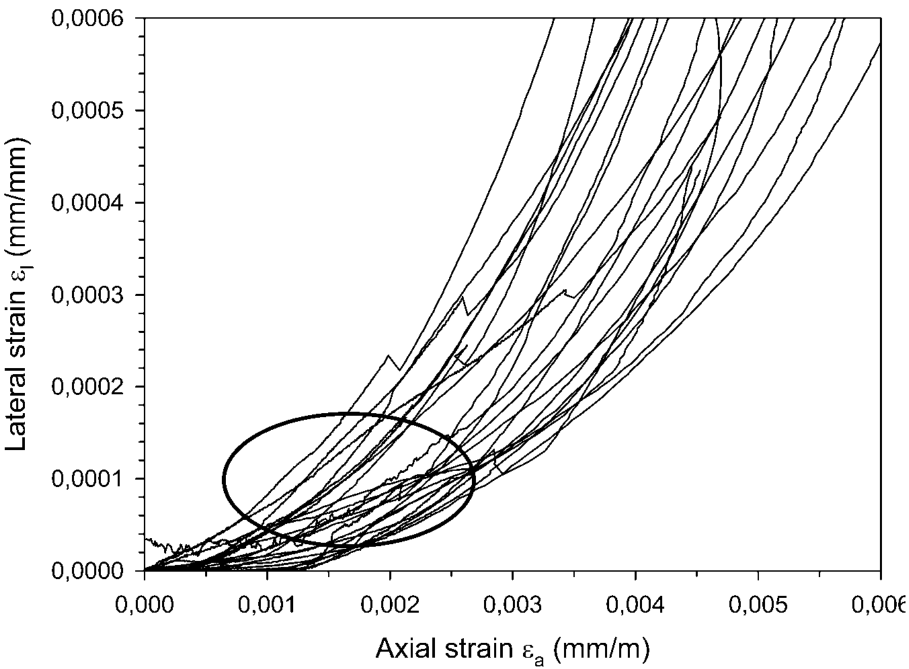

Fig. 6. Lateral vs. axial strain curves for estimating the critical extension strain.

SED
5, 897–916, 2013

Time dependent effects on mine stability

M. Alber

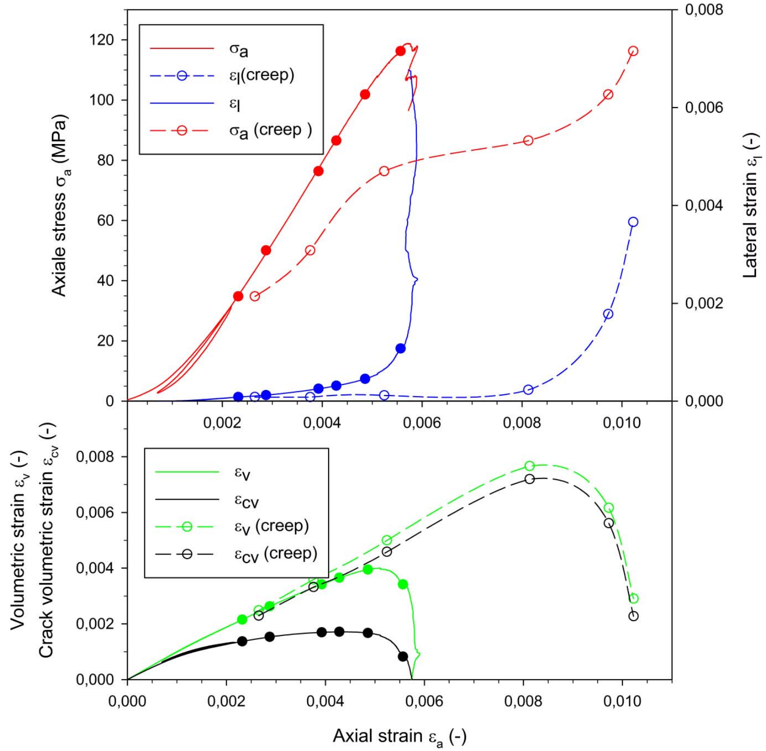

Fig. 7. Comprehensive graph showing stress-strain data of a UCS test (solid lines) and creep test (dashed lines) on sandstones from the same layer of the hanging wall in the mine.

SED
5, 897–916, 2013

Time dependent effects on mine stability

M. Alber

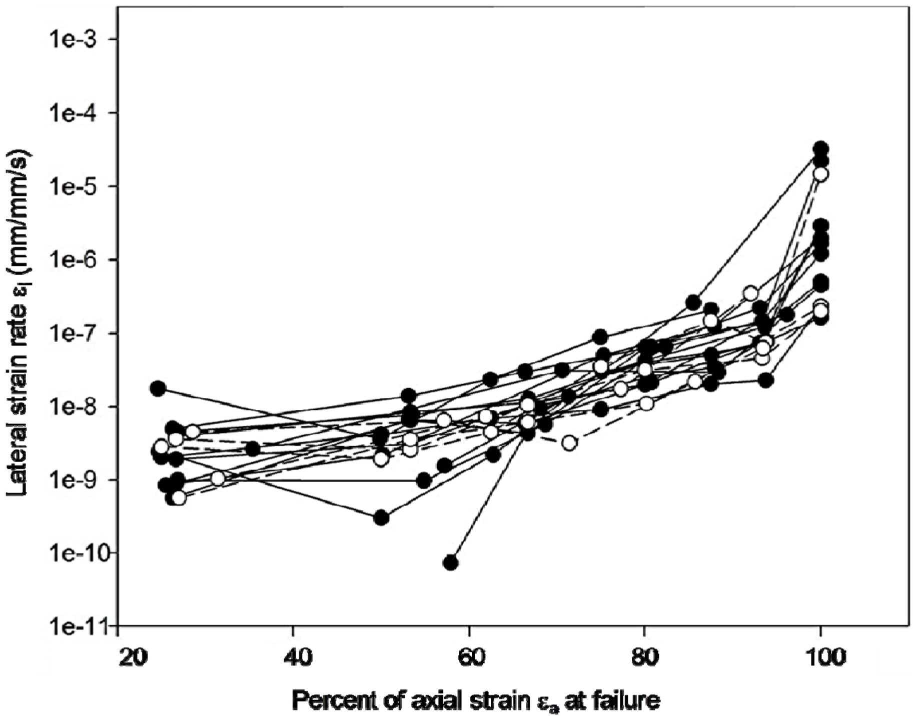

Fig. 8. Lateral strain rates as a function of axial strain levels for sandstone from the Ruhr mining district (Hellenkamp, 2011). Data from multistage creep tests on intact sandstones (black dots) and pre-damaged (open dots) sandstones from the mine.

SED
5, 897–916, 2013